# Spin-chirality separation and $S_3$ symmetry breaking in the magnetization plateau of the quantum spin tube

Kouichi Okunishi,[1] Masahiro Sato,[2] Tôru Sakai,[3,4] Kiyomi Okamoto,[5] and Chigak Itoi[6]
[1]*Department of Physics, Niigata University, Niigata 950-2181, Japan*
[2]*Department of Physics and Mathematics, Aoyama Gakuin University, Sagamihara, Kanagawa 252-5258, Japan*
[3]*Japan Atomic Energy Agency, SPring-8, Sayo, Hyogo 679-5148, Japan*
[4]*Department of Material Science, University of Hyogo, Kamigori, Hyogo 678-1297, Japan*
[5]*Department of Physics, Tokyo Institute of Technology, Meguro-ku, Tokyo 152-8551, Japan*
[6]*Department of Physics, Nihon University, Kanda-Surugadai, Chiyoda-ku, Tokyo 101-8308, Japan*
(Received 29 August 2011; revised manuscript received 30 January 2012; published 14 February 2012)

We study the magnetization plateau state of the three-leg spin-$\frac{1}{2}$ tube in the strong rung coupling region, where $S_3$ symmetry breaking and the low-energy chirality degree of freedom play crucial roles. On the basis of the effective chirality model and density matrix renormalization group, we clarify that, as the leg coupling increases, the chirality liquid with gapless nonmagnetic excitations, the spin-imbalance phase, and the vector-spin-chirality ordered phase emerge without closing the plateau spin gap. The relevance of these results to experiments is also discussed.

DOI: 10.1103/PhysRevB.85.054416 PACS number(s): 75.10.Jm, 75.10.Pq, 75.30.Kz, 75.40.Cx

## I. INTRODUCTION

Geometrical frustration on magnetism has long been one of the attractive subjects in condensed-matter and statistical physics, since the frustration provides rich physical phenomena and various ordered/disordered states.[1] It is well-established that the spin chirality often plays a fundamental role as we probe the frustration effects, especially in the triangular lattice systems.[2,3] Recently, multiple-spin orders without any magnetic moment, including vector spin chiral order, have been actively studied as a new topic in frustrated magnetism (e.g., one- and two-dimensional $J_1$-$J_2$ spin models).[4–7] The vector spin chirality also attracts extensive attention in the context of multiferroics,[8] where the chirality order induces electric polarization. In the most of frustrated systems like the $J_1$-$J_2$ models, however, the chirality excitation is usually embedded in conventional magnetic excitations, which make direct observation of the chirality difficult. In order to gain deeper understanding of the frustration physics, thus, it may be a key issue to extract the chirality excitation energetically separated from the magnetic fluctuations in a realistic situation.

Among a mount of frustrating systems, the three-leg spin tube, consisting of coupled three spin-$\frac{1}{2}$ antiferromagnetic chains [see Fig. 1(a)], is one of the models deeply related to spin chirality; We can define clockwise/anticlockwise rotation along the rung in the spin tube. In fact, the topological structure of the spin tube is known to induce several interesting phenomena.[9–20] Recently, spin-tube materials such as $[(CuCl_2tachH)_3Cl]Cl_2$[21,22] and $CsCrF_4$[23,24] have been synthesized and characteristic properties to the spin tube have been revealed by several experimental approaches. In particular, it is pointed out that the broad peak of specific heat is associated with a gapful chirality excitation in the *twisted* tube $[(CuCl_2tachH)_3Cl]Cl_2$.[22] However, it should be also noted that the contribution from gapless magnetic excitation overlaps this broad peak related to chirality.

In this paper, we demonstrate that the quantum phase transitions associated with the chirality actually occur in the magnetization plateau of the *straight* quantum spin tube, where energy scale of the chirality is certainly separated from gapful magnetic excitations. The Hamiltonian of the spin tube is given by

$$\mathcal{H} = \sum_{i=1}^{3}\sum_{j=1}^{L}[J\boldsymbol{S}_{i,j}\boldsymbol{S}_{i+1,j} + J'\boldsymbol{S}_{i,j}\boldsymbol{S}_{i,j+1}] - H\sum_{i,j} S^z_{i,j}, \quad (1)$$

where $\boldsymbol{S}_{i,j}$ is the spin-$\frac{1}{2}$ matrix, $J(J') > 0$ is the intra- (inter-) triangle coupling, and $i$ ($j$) represents the label of the rung (leg) direction ($i$: mod 3). This model looks very simple, but the frustration due to the tube structure is expected to induce various characteristic properties. In fact, it was shown that the model (1) has a uniform vector spin chirality order in the weak rung-coupling region ($J \ll J'$) in a magnetic field $H$.[12,13] A rather interesting parameter region is the strong-coupling limit ($J \gg J'$), where the system is basically described by the weakly coupled triangles. In the strong rung limit, the composite spin

$$\boldsymbol{T}_j = \boldsymbol{S}_{1,j} + \boldsymbol{S}_{2,j} + \boldsymbol{S}_{3,j} \quad (2)$$

on each unit triangle is classified into $T = \frac{3}{2} \oplus \frac{1}{2} \oplus \frac{1}{2}$ sectors and then the $T^z = \frac{1}{2}$ states of $T = \frac{1}{2}$ sectors lead to a robust magnetization plateau at $\frac{1}{3}$ of the full moment.[11] A key point is that the twofold degeneracy of $T = \frac{1}{2}$ sectors in this plateau state brings an active low-energy variable, which is just the chirality degree of freedom. Utilizing the low-energy effective model and density matrix renormalization group (DMRG), we will show that the energetic separation of the spin and chirality excitations leads to nontrivial quantum phase transitions without destroying the magnetization plateau. The main results are summarized in Fig. 1(b); we find chirality liquid, spin imbalance, and the ferrochirality ordered phases. We also explain that these orders are accompanied by $S_3$ symmetry breaking in the unit triangle.

The remaining part of this paper is organized as follows. In Sec. II, we study the $\frac{1}{3}$ plateau state based on the effective spin chirality model. We also discuss the role of $S_3$ symmetry in the quantum spin tube. Section III is devoted to the

 

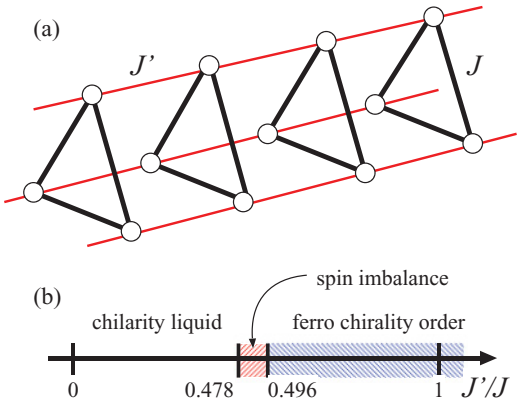


FIG. 1. (Color online) (a) Structure of the three-leg spin tube and (b) ground-state phase diagram of the $\frac{1}{3}$ plateau state of the spin tube. The plateau is predicted to vanish at a strong leg-coupling point $J/J' \sim 0.1$[11,12] (see the text).

numerical results derived from the DMRG method. Combining the DMRG results with the analytical predictions in Sec. II, we reveal three new phases in the plateau region: chirality liquid, spin imbalance, and the ferrochirality ordered phases. Finally, we summarize our result and the relation between it and previous studies in Sec. IV. Furthermore, we discuss the relevance of our result to experiments.

## II. EFFECTIVE CHIRALITY MODEL AND $S_3$ SYMMETRY

Let us start with the low-energy effective theory for the plateau state in the strong rung-coupling region. We can represent the twofold degenerating bases for the $T^z = 1/2$ states of $T = \frac{1}{2}$ on each triangle as

$$|L\rangle = (|\downarrow\uparrow\uparrow\rangle + \omega|\uparrow\downarrow\uparrow\rangle + \omega^{-1}|\uparrow\uparrow\downarrow\rangle)/\sqrt{3}, \quad (3a)$$

$$|R\rangle = (|\downarrow\uparrow\uparrow\rangle + \omega^{-1}|\uparrow\downarrow\uparrow\rangle + \omega|\uparrow\uparrow\downarrow\rangle)/\sqrt{3}, \quad (3b)$$

where $\omega = e^{2\pi i/3}$ and $L$ ($R$) denotes the left- (right-) handed mode in the rung direction.[9] These two states indeed stand for the chirality degree of freedom. By projecting out the high-energy states with $T^z = -\frac{1}{2}$ and $T = \frac{3}{2}$ in every unit triangle, the effective Hamiltonian of the plateau state is obtained as

$$\mathcal{H}_{\rm eff} = \sum_j \Big[ \frac{K_{xy}}{2}(\tau_j^+\tau_{j+1}^- + \tau_j^-\tau_{j+1}^+) + K_z\tau_j^z\tau_{j+1}^z + \frac{K'_{xy}}{2}(\tau_{j-1}^+\tau_{j+1}^- + \tau_{j-1}^-\tau_{j+1}^+) + \frac{K_3}{4}(\tau_{j-1}^+\tau_j^+\tau_{j+1}^+ + \tau_{j-1}^-\tau_j^-\tau_{j+1}^-)\Big], \quad (4)$$

where $\boldsymbol{\tau}_j$ is the pseudospin-$\frac{1}{2}$ matrix defined by $\tau_j^z = (|L\rangle_{jj}\langle L| - |R\rangle_{jj}\langle R|)/2$. The coupling constants are evaluated as $K_{xy} = 2J'/3 - 5J'^2/(27J)$, $K_z = -J'^2/J$, $K'_{xy} = 8J'^2/(27J)$, and $K_3 = -16J'^2/(27J)$ within the second-order perturbation in $J'$. Here, it is worth noting that the relation between $\boldsymbol{\tau}_j$ and $\boldsymbol{S}_{i,j}$ is given by $\tau_j^z = \sqrt{3}\hat{P}_j\chi_j\hat{P}_j$ and $\tau_j^x = -\hat{P}_j\mu_j\hat{P}_j$, where

$$\chi_j = \sum_{i=1}^{3}(\boldsymbol{S}_{i,j} \times \boldsymbol{S}_{i+1,j})^z/3, \quad (5a)$$

$$\mu_j = S_{1,j}^z - \big(S_{2,j}^z + S_{3,j}^z\big)/2, \quad (5b)$$

are, respectively, the $z$ component of the vector spin chirality and an imbalanced magnetization on each triangle and $\hat{P}_j = |L\rangle_{jj}\langle L| + |R\rangle_{jj}\langle R|$ is the projection operator to the $T_j^z = \frac{1}{2}$ states of $T = \frac{1}{2}$.

In order to resolve possible quantum phase transitions, it is very instructive to discuss the discrete symmetry of the spin tube. The spin tube has $S_3$-group ($\cong C_{3v}$ point group) symmetry in the rung direction in addition to the translational symmetry along the leg direction. The operations in the $S_3$ group are composed of the cyclic permutation $\boldsymbol{S}_{i,j} \to \boldsymbol{S}_{i+1,j}$ with mod 3 and the reflection $\boldsymbol{S}_{i,j} \leftrightarrow \boldsymbol{S}_{i',j}$ at a bond in every unit triangle ($i \neq i'$). Possible $S_3$ symmetry breakings are classified by its subgroups: (a) the bond-parity breaking with conserving the cyclic symmetry, (b) the cyclic $Z_3$ symmetry breaking with conserving a part of bond-party symmetry, or (c) the full breaking of the $S_3$ symmetry. The vector spin chirality $\chi_j$ is a typical order parameter in the case (a), which changes its sign by the reflection but is invariant under the cyclic permutation. This cyclic symmetry is related to the spin current circulating in the rung direction. On the other hand, $\mu_j$ can be an order parameter of the case (b), since its form changes via the cyclic permutation but is invariant under the reflection $\boldsymbol{S}_{2,j} \leftrightarrow \boldsymbol{S}_{3,j}$. If $\mu_j$ becomes finite, it suggests that the isosceles-triangle-type imbalance occurs for $\langle S_{i,j}^z\rangle$ in the plateau state.

We discuss the relation between the $S_3$ symmetry and the effective model (4). Write the cyclic permutation operation of the $S_3$ symmetry group as $\mathcal{T}_c$, and the bond reflection as $\mathcal{T}_r(=\mathcal{T}_r^{-1})$. In the level of the effective chirality $\boldsymbol{\tau}$, the $S_3$ symmetric operation is given by

$$\mathcal{T}_c\tau_j^z\mathcal{T}_c^{-1} = \tau_j^z, \quad \mathcal{T}_c\tau_j^+\mathcal{T}_c^{-1} = \omega\tau_j^+, \quad \mathcal{T}_c\tau_j^+\mathcal{T}_c^{-1} = \omega^2\tau_j^+,$$
$$\mathcal{T}_r\tau_j^z\mathcal{T}_r = -\tau_j^z, \quad \mathcal{T}_r\tau_j^+\mathcal{T}_r = \tau_j^-, \quad \mathcal{T}_r\tau_j^-\mathcal{T}_r = \tau_j^+ \quad (6)$$

for any $j$. Under these operations of the $S_3$ symmetry, the effective Hamiltonian (4) is confirmed to be invariant. Here we should remark that in the model of Eq. (4), the second-roder perturbation process generates the U(1) symmetry-breaking $K_3$ term, although the U(1)-symmetric XY model, which is obtained within the first-order perturbation, has been often used for the spin tubes.[10,14,19] This is consistent with the fact that $\tau_j^z \sim \chi_j$ is not exactly conserved in the original spin tube. Thus, we need to careful consider the role of symmetry and interactions in the effective model (4).

According to the bosonization approach,[25] the low-energy physics of the model (4) is described by a massless free boson theory with several interactions. The effective Hamiltonian for the free boson, i.e., the Tomonaga-Luttinger (TL) liquid, is represented as

$$\mathcal{H}_{\rm TL} = \int dx \frac{v}{2}[\tilde{K}(\partial_x\theta)^2 + \tilde{K}^{-1}(\partial_x\phi)^2], \quad (7)$$

where $(\phi,\theta)$ is the canonical pair of scalar fields ($x = ja$ and $a$ is lattice spacing), $\tilde{K}$ is the TL-liquid parameter, and $v$ is the low-energy excitation velocity of the model of Eq. (4). The effective spin $\boldsymbol{\tau}_j$ and the bosonic fields $(\phi,\theta)$ are related as

$$\begin{aligned} \tau_j^z &\simeq \frac{a}{\sqrt{\pi}}\frac{\partial\phi(x)}{\partial x} + (-)^j a_1 \cos\sqrt{4\pi}\phi(x) + \cdots, \\ \tau_j^+ &\simeq e^{i\sqrt{\pi}\theta(x)}[(-)^j b_0 + b_1 \cos\sqrt{4\pi}\phi(x) + \cdots], \end{aligned} \tag{8}$$

with nonuniversal constants $a_1$, $b_0$, and $b_1$. The $S_3$ symmetry operations on the effective fields are summarized as

$$\begin{aligned} &\mathcal{T}_r\theta(x)\mathcal{T}_r = -\theta(x), \quad \mathcal{T}_r\phi(x)\mathcal{T}_r = -\phi(x) + \sqrt{\pi}/2, \\ &\mathcal{T}_c\theta(x)\mathcal{T}_c^{-1} = \theta(x) + 2\sqrt{\pi}/3. \end{aligned} \tag{9}$$

In addition, the operation of one-site translation along the leg $\mathcal{T}_l$ transforms the boson fields as

$$\begin{aligned} \mathcal{T}_l\theta(x)\mathcal{T}_l^{-1} &= \theta(x+a) + \sqrt{\pi}, \\ \mathcal{T}_l\phi(x)\mathcal{T}_l^{-1} &= \phi(x+a) + \sqrt{\pi}/2. \end{aligned} \tag{10}$$

These symmetries impose significant restriction to the possible interaction terms in the effective field theory. Among various vertex operators permitted by the $S_3$ and translational symmetries, the most relevant terms are given by for $\cos(2\sqrt{2\pi}\phi)$ and $\cos(6\sqrt{\pi}\theta)$, for which the scaling dimensions are, respectively, $4\tilde{K}$ and $9/\tilde{K}$. Since the value of $\tilde{K}$ approaches unity in the $J'/J \to 0$ limit (the XY model), we can see that the interaction terms in Eq. (4) are all irrelevant for sufficiently small $J'$, suggesting that the critical chirality liquid is realized in a certain region of small $J'$. On the other hand, the system may have two kind of instabilities as $J'$ increases. The first case is the ferrochirality order of $\tau_j^z \sim \chi_j$. Since the negative $K_z$ in Eq. (4) raises the value of $\tilde{K}$ to $+\infty$, the ferromagnetic instability may occur, at which the velocity $v$ also vanishes. The other case is the *staggered* order of the imbalanced magnetization $\mu_j$; if $9/\tilde{K} < 2$, the $\theta$ field is locked and then the staggered component of $\tau_j^x$ can have a finite expectation value through the relation $\hat{P}_j\mu_j\hat{P}_j = -\tau_j^x \sim (-)^j\cos(\sqrt{\pi}\theta)$. Here, we note that, in the following numerical computations, the ferrochirality order actually appears, but a uniform order of $\mu_j$ is realized rather than the staggered type.

## III. NUMERICAL RESULTS

We now apply DMRG to the spin-tube model (1) to quantitatively examine the transitions and orderings with the help of results in Sec. II. We fix $J = 1$ in the following numerical calculations.

### A. Chirality liquid phase

First, we focus on a sufficiently strong-rung coupling region. In Fig. 2, we present the longitudinal spin correlation function $\langle S_{i,j}^z S_{i,j'}^z\rangle$ for $L = 96$ systems with $J' = 0.01, \ldots,$ 0.45. The rapid decay near the right edge in Fig. 2 comes from the open boundary effect. Thus, it can be confirmed that the correlation function follows a power-law decay for $|j - j'| \lesssim 50$: $\langle S_{i,j}^z S_{i,j'}^z\rangle - m^2 \sim (-)^{j-j'}|j - j'|^{-\eta}$, where $m = \frac{1}{6}$ is the uniform magnetization per spin and $\eta$ is the critical exponent. This decay fashion is in agreement with the prediction from the effective TL-liquid theory (7). We can also see that $\eta$ becomes close to 0.5 in the $J' = 0$ limit, where Eq. (4) reduces to the XY model. As $J'$ increases, $\eta$ approaches zero toward the ferrochirality transition. Utilizing the effective field theory (7) based on Eq. (4), we can evaluate the critical exponent $\eta$ in the strong rung-coupling region $J \gg J'$. The value to the second order of $J'$ is given by $\eta \simeq 0.5 - 0.885J' + 0.640J'^2 + \cdots$, where we have assumed the nonuniversal parameter $b_0 = 0.5424\cdots$.[26] We have confirmed that this value of $\eta$ is semiquantitatively consistent with the numerically estimated value from the correlation function of Fig. 2 in $J \gg J'$. From these results, we conclude that the gapless nonmagnetic chirality excitation is described by the effective model of Eq. (4). Here, note that the width of the plateau is sufficiently large for $J' < 0.5$ and the transverse correlator $\langle S_{i,j}^x S_{i,j'}^x\rangle$ exponentially decays, indicating that the magnetic excitation has a large gap corresponding to the plateau width.

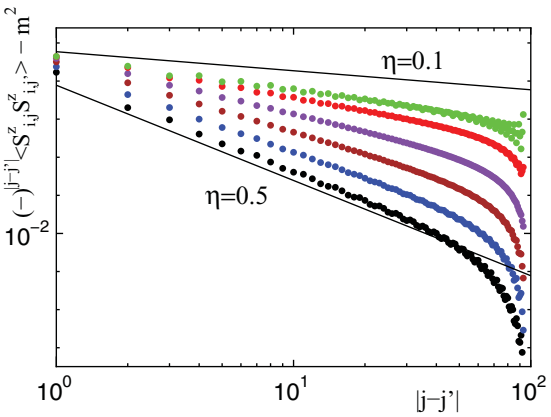


FIG. 2. (Color online) Longitudinal spin correlation function $\langle S_{i,j}^z S_{i,j'}^z\rangle$ of the spin tube for $J' = 0.01$, 0.1, 0.2, 0.3, 0.4, and 0.45 from bottom to top, where $m = \frac{1}{6}$. Two solid lines indicate guides for $\eta = 0.5$ (XY chain) and 0.1.

### B. Ordered phases

As $J'$ further increases, the negative $K^z$ derives the system toward a ferrochirality ordered state with $\langle\chi_j\rangle \neq 0$. Figure 3 illustrates the results of the order parameters $\chi = \langle\chi_j\rangle$ and $\mu = \langle\mu_j\rangle$. Here, $\chi$ is observed at the center triangle of the tube of size $L = 120$[5] and $\mu$ is the bulk expectation value based on the infinite system DMRG. We have checked that the boundary effect is negligible within computations for $L = 96, 120$, and 144. From the main panel, we can see two quantum phase transitions near $J' = 0.5$. Note that the plateau width around $J' = 0.5$ is about $0.5J$, which is sufficiently larger than the energy scale of the nonmagnetic chirality excitation. Figure 3 clearly shows the emergence of the ferro-chirality order in $J' > J'_{c2} = 0.496$, which is consistent with the effective model (4). We have confirmed that this ferrochirality order extends to $J' > 1$ and, thus, it would be adiabatically connected to the vector chirality order in the region of the weakly coupled three chains.[12] Here, note that both $\langle S_{i,j}^x S_{i,j'}^x\rangle$ and $\langle S_{i,j}^z S_{i,j'}^z\rangle$ show exponential decays in $J' > J'_{c2}$ and, thus, the magnetic and chirality excitations have finite gaps in this chirality ordered phase.

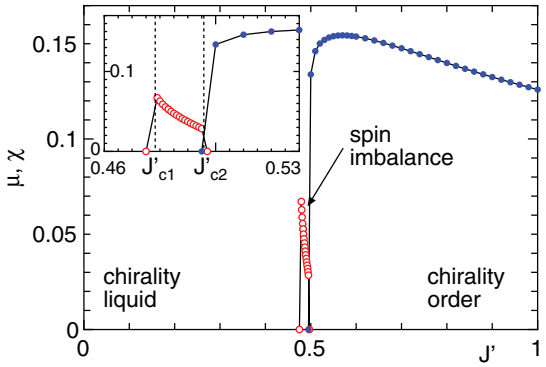


FIG. 3. (Color online) Expectation value of the order parameters $\chi$ (solid circle) and $\mu$ (open circle). (Inset) The order parameters around the transition points. The vertical broken lines indicate the transition points $J'_{c1}$ and $J'_{c2}$.

From the inset of Fig. 3, we also find that the spin-imbalance phase emerges in a narrow region $J'_{c1} < J' < J'_{c2}$ with $J'_{c1} \simeq 0.478$. In this region, the symmetry of the unit triangle reduces to the isosceles type, where the expectation value of one spin of each rung triangle is larger than those of the remaining two spins: $\langle S^z_{i,j}\rangle > \langle S^z_{i+1,j}\rangle = \langle S^z_{i+2,j}\rangle$. In Fig. 4, we present the $\langle S^z_{i,j}\rangle$ distribution for $J' = 0.485$, which exhibits a typical spin profile of the spin-imbalance state. The open-boundary effect rapidly decays and a uniform spin imbalance along the chain direction is realized around the center of the tube. Figure 5 shows a semilog plot of $\langle S^z_{i,j} S^z_{i,j'}\rangle - m_i^2$, where $m_i$ is the bulk expectation value of $S^z_{i,j}$ calculated at the center of the tube. The exponential decay of the correlation functions in Fig. 5 indicates that the system is gapful. We note that the imbalanced nature is present not only in the magnetization profile but also in the spin correlation functions. As we see from the inset of Fig. 5, the correlation length for the less polarized spins becomes divergent as $J' \to J'_{c1} + 0$, while that for the most polarized spin remains finite value. This suggests that the instability of the spin imbalance toward the chirality liquid state ($J' < J'_{c1}$) may be governed by the fluctuation of the less

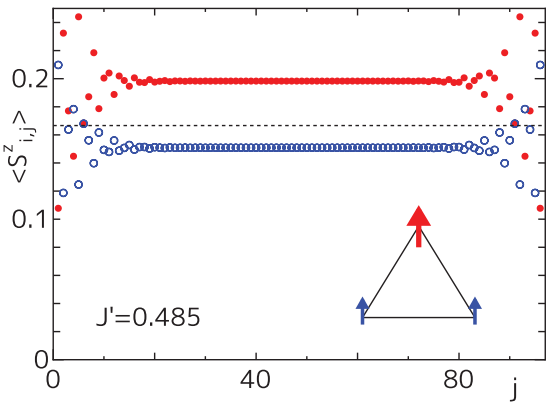


FIG. 4. (Color online) Spin profile $\langle S^z_{i,j}\rangle$ of the spin-imbalance phase. The tube length is $L = 96$ and the intertriangle coupling is $J' = 0.485$. Solid circles denote the expectation value of the most polarized spin in each rung triangle and the open circles correspond to those of remaining two spins on the triangle. The horizontal broken lines is the averaged magnetization of each rung in the plateau state.

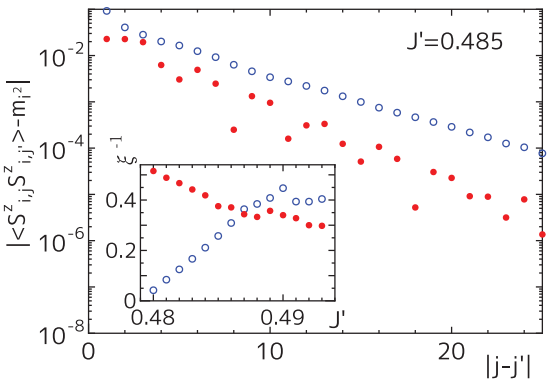


FIG. 5. (Color online) Correlation function $|\langle S^z_{i,j} S^z_{i,j'}\rangle - m_i^2|$ in the spin-imbalance phase. The solid circles is the correlator for the chain consisting of the most polarized spins on the unit triangles, and the open circles correspond to that for the remaining two chains. (Inset) The $J'$ dependence of the inverse correlation length $\xi^{-1}$ along the chains for the most and less polarized spins in the triangle.

polarized spins of the triangle, although the critical behavior of $\mu$ cannot be determined within the accuracy of the present DMRG results. As $J'$ increases, the correlation lengths of the most polarized spin and the remaining two become comparable with each other and finally arrive at the ferrochirality transition point $J'_{2c}$. Here, we note that, for $0.485 \lesssim J' < J'_{c2}$, the spin correlation functions becomes highly oscillating and, thus, precise estimation of the correlation length is difficult. We stress that this imbalanced order cannot be described by the effective model [Eq. (4)]. This suggests that the hybridization of $T^z = 3/2$ sector plays an essential role in the imbalanced phase (see the following paragraphs). On the other hand, the jump of the order parameters at $J'_{c2}$ clearly shows that the transition at $J' = J'_{c2}$ is of first order, where the two different symmetry breakings are switched.

Let us discuss the nature of the spin-imbalance phase in more detail. As we discussed above, the imbalanced order is uniform along the leg direction, while the field theory based on the effective model (4) suggests the emergence of a staggered imbalance order ($\langle \mu_j\rangle = -\langle \mu_{j+1}\rangle$). This mismatch of the effective theory may be attributed to the fact that the imbalanced order is located at very vicinity of the ferrochirality transition point $J'_{c2}$, where the velocity $v$ almost vanishes and, thus, the system becomes fragile. Furthermore, we find that the rapid increase of $\mu$ in $J' > J'_{c1}$ causes a rapid raise of the energy of the unit triangle (DMRG data are not presented here), implying that the effect of $J'$ nonperturbatively reduces the energy of the intratriangle bonds. Thus, it is suggested that the role of the intratriangle coupling becomes essential and, thus, the $T = \frac{3}{2}$ sector certainly hybridizes into the plateau state in the spin-imbalance phase.

The effective model (4) is based on the massive weight of the $T = \frac{1}{2}$ sector, while the mixing of the $T = \frac{3}{2}$ sector is possibly essential for the spin-imbalance phase. We should, thus, investigate the expectation value of $\hat{P}^{1/2}_j = (\boldsymbol{T}^2_j/3 - 5/4)$, which is the projection operator into the $T = \frac{1}{2}$ sector. In the $J' = 0$ limit, $\langle \hat{P}^{1/2}_j\rangle = 1$ and it gradually decreases up to $J'_{c1}$. Figure 6 shows $\langle \hat{P}^{1/2}\rangle$ around the transition points, which

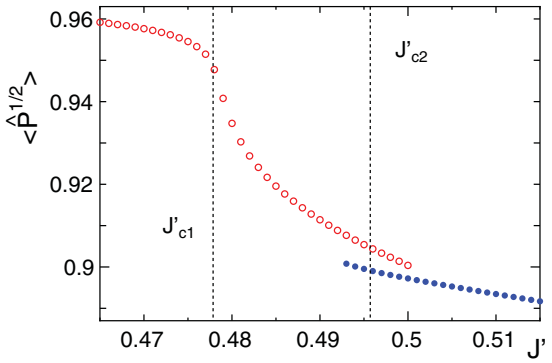


FIG. 6. (Color online) Expectation value of the projection operator $\langle \hat{P}^{1/2} \rangle$ on the unit triangle.

is obtained by the infinite DMRG. In the figure, we can see that the behavior of $\langle \hat{P}^{1/2} \rangle$ drastically changes at $J_{c1} \simeq 0.478$ and $J_{c2} = 0.496$. In $J_{c1} < J' < J_{c2}$, $\langle \hat{P}^{1/2} \rangle$ rapidly decreases with increasing $J'$. This supports that the driving mechanism of the spin-imbalance phase relies on the mixing of the $T = \frac{3}{2}$ sector. Although a Berezinskii-Kosterlitz-Thouless–type transition accompanying the $Z_3$ symmetry breaking[27] is naively expected at $J_{c1}$, the nature of the phase transition might be essentially modified by the $T = \frac{3}{2}$ sector. However, we may claim within the present analysis that $\langle \hat{P}^{1/2} \rangle$ is continuously changed around $J_{c1}$, suggesting a continuous quantum phase transition. Further analysis is necessary to completely determine the nature of this transition, including the universality class. On the other hand, there exists a clear jump of $\langle \hat{P}^{1/2} \rangle$ at $J_{c2} = 0.496$. The two branches near $J_{c2}$ represent two self-consistent solutions corresponding to the chirality ordered and spin-imbalance states in the DMRG iterations; the solution of the previous parameter is used as an initial state for the next parameter, so the metastable states can be reproduced. By comparing energies of the two branches, the first-order transition point can be determined as $J'_{c2} \simeq 0.496$. This result is consistent with the behaviors of the order parameters in Fig. 3.

## IV. CONCLUSIONS AND DISCUSSIONS

In conclusion, we have explored the quantum phase transitions of the $\frac{1}{3}$ plateau state of the spin tube. In contrast to the usual plateaus of one-dimensional spin systems (chains and ladders), the chirality degree of freedom generated from the tube structure plays crucial roles. The results are summarized in Fig. 1(b), where the chirality liquid phase with gapless nonmagnetic excitations, the spin-imbalance phase, and the ferrochirality phase emerge. The qualitative features of these phases may be explained by the effective chirality model (4) and the $S_3$ symmetry breakings. However, the precise analysis of the projection operator $\hat{P}^{1/2}$ has revealed that the uniform spin-imbalance order is driven by mixing of the $T = \frac{3}{2}$ sector, which is beyond the scope of the effective model (4). The transition between the chirality liquid and the spin-imbalance phase is of continuous type, and the fluctuation of less polarized spins in the imbalance phase becomes divergent near the transition. On the other hand, the transition between the spin-imbalance and ferrochirality ordered phases is shown to be of first-order type.

Here it should be noted that another spin-imbalance phase with gapless magnetic excitations is expected in a high magnetic field.[13] Its connection to the present spin-imbalance phase may be an interesting problem for thorough understanding of the mechanisms of spin imbalance. As mentioned in the Introduction, a chirality-ordered spin liquid appears in the weak rung-coupling region $J \ll J'$ in magnetic fields.[12] This spin liquid is expected to change into the 1/3 plateau state with the chirality order[12] via a BKT transition[11] at the order of $J/J' = 0.1$. Combining our present results with this, we can conclude that, as $J'$ increases from the strong rung limit, the chirality liquid, spin-imbalance order, ferrochirality order, and ferrochirality-ordered spin liquid can be observed at $m = \frac{1}{6}$ in order.

An important aspect of the spin tube is that the phase transitions occur without destroying the plateau. The energy scale of the chirality is significantly lower than the width of the large plateau. Therefore, for example, a specific heat measurement will solely observe a linear temperature dependence originating from the chirality modes in the wide spin-gapped plateau region of $J' < J'_{c1}$, in contrast to the twisted tube.[22] From an experimental viewpoint, moreover, another plausible feature of the spin tube is that the gapped chirality order is expanded in the wide range of $J'$, which is contrasted to the narrow chirality-ordered phases with gapped magnetic excitations in the classical XY model on triangular lattice[2] and spin-$S$ $J_1$-$J_2$ chains.[28,29] If a coupling between chirality and electric polarization is introduced, the chirality order can induce a ferroelectric polarization in spite of the absence of any magnetic ordering. Also, the similar chirality degree of freedom is discussed in the coupled trimer model, which may reduce to the spin tube in an anisotropic limit.[30] We, thus, believe that the spin tube provides a fascinating playground for chirality degrees in the realistic experimental situation.

## ACKNOWLEDGMENTS

This work has been partly supported by Grants-in-Aid for Scientific Research (Grants No. 23340109, No. 23540442, No. 21740295, and No. 23540388) and Priority Area "Novel States of Matter Induced by Frustration" (Grants No. 22014012 and No. 22014016) from MEXT, Japan. Numerical computations were partly performed at the Supercomputer Center, ISSP, University of Tokyo, and the Computer Room, Yukawa Institute, Kyoto University.

[1] For example, *Frustrated Spin Systems*, edited by H. T. Diep (World Scientific, Singapore, 2005).
[2] S. Miyashita and H. Shiba, J. Phys. Soc. Jpn. **53**, 1145 (1984).
[3] H. Kawamura, J. Phys. Condens. Matter **10**, 4707 (1998).
[4] N. Shannon, T. Momoi, and P. Sindzingre, Phys. Rev. Lett. **96**, 027213 (2006).
[5] K. Okunishi, J. Phys. Soc. Jpn. **77**, 114004 (2008).

[6]T. Hikihara, L. Kecke, T. Momoi, and A. Furusaki, Phys. Rev. B **78**, 144404 (2008).
[7]S. Furukawa, M. Sato, and S. Onoda, Phys. Rev. Lett. **105**, 257205 (2010).
[8]K. F. Wang, J.-M. Liu, and Z. F. Ren, Adv. Phys. **58**, 321 (2009).
[9]H. J. Schulz, in *Correlated Fermions and Transport in Mesoscopic Systems*, edited by T. Martin, G. Montambaux, and J. Tran Than Van (1996); e-print arXiv:cond-mat/9605075.
[10]K. Kawano and M. Takahashi, J. Phys. Soc. Jpn. **66**, 4001 (1997).
[11]D. C. Cabra, A. Honecker, and P. Pujol, Phys. Rev. Lett. **79**, 5126 (1997); Phys. Rev. B **58**, 6241 (1998).
[12]M. Sato, Phys. Rev. B **75**, 174407 (2007).
[13]M. Sato and T. Sakai, Phys. Rev. B **75**, 014411 (2007).
[14]A. Luscher, R. M. Noack, G. Misguich, V. N. Kotov, and F. Mila, Phys. Rev. B **70**, 060405(R) (2004).
[15]T. Sakai, M. Sato, K. Okunishi, Y. Otsuka, K. Okamoto, and C. Itoi, Phys. Rev. B **78**, 184415 (2008).
[16]S. Nishimoto and M. Arikawa, Phys. Rev. B **78**, 054421 (2008).
[17]T. Sakai, M. Sato, K. Okunishi, K. Okamoto, and C. Itoi, J. Phys. Condens. Matter. **22**, 403201 (2010).
[18]K. Okunishi, S. Yoshikawa, T. Sakai, and S. Miyashita, Prog. Theor. Phys. Suppl. **159**, 297 (2005).
[19]J.-B. Fouet, A. Läuchli, S. Pilgram, R. M. Noack, and F. Mila, Phys. Rev. B **73**, 014409 (2006).
[20]M. Lajko, P. Sindzingre, and K. Penc, Phys. Rev. Lett. **108**, 017205 (2012).
[21]J. Schnack, H. Nojiri, P. Kögerler, G. J. T. Cooper, and L. Cronin, Phys. Rev. B **70**, 174420 (2004).
[22]N. B. Ivanov, J. Schnack, R. Schnalle, J. Richter, P. Kögerler, G. N. Newton, L. Cronin, Y. Oshima, and H. Nojiri, Phys. Rev. Lett. **105**, 037206 (2010).
[23]H. Manaka, Y. Hirai, Y. Hachigo, M. Mitsunaga, M. Ito, and N. Terada, J. Phys. Soc. Jpn. **78**, 093701 (2009).
[24]H. Manaka, T. Etoh, Y. Honda, N. Iwashita, K. Ogata, N. Terada, T. Hisamatsu, M. Ito, Y. Narumi, A. Kondo, K. Kindo, and Y. Miura, J. Phys. Soc. Jpn. **80**, 084714 (2011).
[25]See, for example, T. Giamarchi, *Quantum Physics in One Dimension* (Oxford University Press, Oxford, 2004).
[26]T. Hikihara and A. Furusaki, Phys. Rev. B **69**, 064427 (2004).
[27]K. Nomura, J. Phys. A: Math. Gen. **28**, 5451 (1995).
[28]T. Hikihara, M. Kaburagi, and H. Kawamura, Phys. Rev. B **63**, 174430 (2001).
[29]M. Sato, S. Furukawa, S. Onoda, and A. Furusaki, Mod. Phys. Lett. B **25**, 901 (2011); e-print arXiv:1101.1374; S. Furukawa, M. Sato, S. Onoda, and A. Furusaki (to be published).
[30]Y. Kamiya and C. D. Batista, e-print arXiv:1110.4120.